ISSN 1606-867X (Print)
ISSN 2687-0711 (Online)
Condensed Matter and Interphases
Kondensirovannye Sredy i Mezhfaznye Granitsy
https://journals.vsu.ru/kcmf/

Short communication

Short communication
https://doi.org/10.17308/kcmf.2025.27/13021

Infrared synchrotron nanovisualization of a biomimetic layer composed of trimethyldihydroquinoline and nanocrystalline hydroxyapatite

P. V. Seredin[1]✉, D. L. Goloshchapov[1], Y. A. Peshkov[1], N. S. Buylov[1], A. Y. Potapov[1], K. S. Shikhaliev[1], Yu. A. Ippolitov[2], Raul O. Freitas[3], Francisco C. B. Maia[3]

[1]*Voronezh State University, 1 Universitetskaya pl., Voronezh 394018, Russian Federation*

[2]*Voronezh State Medical University, 10 Studentcheskaya st., Voronezh 394036, Russian Federation*

[3]*Brazilian Synchrotron Light Laboratory (LNLS), Brazilian Center for Research in Energy and Materials (CNPEM), Campinas 13083-970, Sao Paulo, Brazil*

Abstract

Objective of the article: This study presents the findings of research on a biomimetic organomineral layer composed of trimethyl-dihydroquinoline, polymerized in the presence of nanocrystalline carbonate-substituted non-stoichiometric hydroxyapatite (n-cHAp).

Experimental part: The morphological features of the biomimetic layer were visualized using synchrotron infrared near-field spectroscopy.

Conclusions: It has been demonstrated that the biomimetic layer formed on the surface of dental enamel exhibits a morphological structure characterized by a uniformly distributed and densely packed composite film of poly(2,2,4-trimethyl-1,2-dihydroquinoline-6,7-diol) and n-cHAp. The resulting dental coating, based on polydihydroquinoline and nanocrystalline hydroxyapatite, possesses a Vickers hardness coefficient comparable to that of healthy enamel.

Keywords: trimethyl-dihydroquinoline, biomimetic layer, dental enamel, near-field infrared spectroscopy, synchrotron radiation

Funding: The study was funded by the Russian Science Foundation, as part of scientific project No. 23-15-00060.

Acknowledgments:

Authors thank the Brazilian Synchrotron Light Laboratory for providing beamtime for SINS and s-SNOM experiments at the Imbuia beamline of Sirius (Proposal 20241295).

For citation: Seredin P. V., Goloshchapov D. L., Peshkov Y. A., Buylov N. S., Potapov A. Yu., Shikhaliev Kh. S., Ippolitov Yu. A., Raul O. Freitas, Francisco C. B. Maia. Infrared synchrotron nanovisualization of a biomimetic layer composed of trimethyldihydroquinoline and nanocrystalline hydroxyapatite. *Condensed Matter and Interphases*. 2025;27(3): 483–489. https://doi.org/10.17308/kcmf.2025.27/13021

Для цитирования: Середин П. В., Голощапов Д. Л., Пешков Я. А., Буйлов Н. С., Потапов А. Ю., Шихалиев Х. С., Ипполитов Ю. А., Raul O. Freitas, Francisco C. B. Maia. ИК-синхротронная нановизуализация биомиметического слоя на основе триметилдигидрохинолина и нанокристаллического гидроксиапатита. *Конденсированные среды и межфазные границы*. 2025;27(3): 483–489. https://doi.org/10.17308/kcmf.2025.27/13021

✉ Pavel V. Seredin, e-mail: paul@phys.vsu.ru

1. Introduction

In the past decade, there has been an exponential increase in interest in dental biomaterials with antimicrobial properties applied to the surfaces of dental tissues in the form of thin films. One promising class of compounds with broad-spectrum antibacterial activity is quinoline and its derivatives [1], which can form homogeneous films [2] with antimicrobial activity [3]. However, there are virtually no reports in the literature on the use of quinolines in dentistry. This lack of research can be attributed to the unsatisfactory adhesion strength of these dental materials to the surfaces of hard dental tissues, as well as their low stability and short functional lifespan.

The first problem can be solved by the incorporation of functional groups into the composition of quinoline derivatives, which allows for the chemical adsorption of the polymer on the surface of the material [4, 5]. As has been repeatedly shown, increasing the stabilization and functioning of such films is possible using nanoparticles of various materials [6]. The strategy of forming dental layers that combine both remineralization functions and antimicrobial properties on the surface of enamel is the optimal solution to this problem [7–9].

At the same time, the formation of biomimetic layers should replicate the biogenic complexity of enamel at the nanoscale, where conjugation within individual crystals occurs via protein chains [10]. Determining the mechanisms of conjugation of organomineral systems at the nanoscale is a complex task requiring the use of a wide range of methods. One possible approach is the use of near-field infrared microscopy coupled with an atomic force microscope [11]. Combining the advantages of these methods allows the determination of the features of molecular conjugation of various compounds while simultaneously recording the topographic arrangement of structural elements of the composite. For enamel apatite, this method allows us to visualize and establish the characteristics of biogenic apatite both during formation and destruction in pathologies at the submicron level [12, 13]. For synthetic nanomaterials based on hydroxyapatite, it becomes possible to identify the features of surface phase formation and the composite hierarchy at the level of individual nanocrystals [14].

In this study, synchrotron near-field infrared nanospectroscopy, combined with atomic force microscopy, was utilized to investigate the organic-mineral interactions and the hierarchical structure of the biomimetic layer formed from the nanopolymer dihydroxyquinoline and nanocrystalline hydroxyapatite.

2. Materials and methods

To create biotemplates, samples of intact human teeth were selected and diagnosed as free of carious lesions in hard tissues based on laser-induced contrast imaging data [15, 16]. Flat, parallel segments of dental tissue were obtained by sectioning the crown of the tooth perpendicularly to the occlusal surface, near the cusp, using the method we proposed earlier [16, 17].

Nanocrystalline carbonate-substituted non-stoichiometric hydroxyapatite, with average nanocrystal sizes of 25×25×50 nm (n-cHAp) [18], was synthesized using a chemical precipitation method [19, 20].

2,2,4-Trimethyl-1,2-dihydroquinoline-6,7-diol hydrobromide (6,7-DiOH-TMDHQ) was synthesized by demethylation of 6,7-dimethoxy-2,2,4-trimethyl-1,2-dihydroquinoline using hydrobromic acid.

To obtain organomineral biomimetic layers, a solution containing n-cHAp in distilled water was prepared [21]. The biotemplate was then introduced into the solution, followed by the immediate addition of 6,7-DiOH-TMDHQ, which initiated an auto-oxidation reaction.

Experiments utilizing infrared scattering scanning near-field optical microscopy (IR s-SNOM) were conducted using equipment of the IMBUIA-nano channel at the Brazilian Synchrotron Light Laboratory (LNLS). A set of quantum cascade lasers (QCL) (MirCat, DRS Daylight Solutions Inc.) was employed, covering a spectral range from 930 to 1730 cm^{-1}, with a minimum frequency step of 1 cm^{-1} for single-frequency excitation. To capture the amplitude and phase of the scattered signal, the optical setup was equipped with a pseudo-heterodyne (psHet) system and an asymmetric Michelson interferometer (neaSNOM, Neaspec GmbH) [22, 23].

The surface morphology and topology of the mineralized biomimetic layer were examined using a scanning electron microscope (SEM) (TESCAN VEGA 3, Czech Republic). Samples were affixed to aluminum microscopic substrates with adhesive carbon tape and subsequently coated with gold (Au) for 120 seconds using a sputtering device from Quorum Techniques Ltd (Q150T).

The mechanical properties of natural mineralized hard tissue and the deposited organomineral layers were analyzed using the Vickers hardness test.

3. Experimental results and discussion

Scanning electron microscopy images of a segment of healthy enamel (biotemplate) and a sample of 6,7-DiOH-PTMDHQ/ n-cHAp are shown in Figures 1a and 1b. The analysis of the local morphology of the natural mineralized tissue (Figure 1a) reveals the oriented growth of enamel prisms [10, 24, 25], which are formed by dense rows of hydroxyapatite nanocrystals, as illustrated in the inset of Figure 1a [26]. In samples with the biomimetic coating of 6,7-DiOH-PTMDHQ/n-cHAp, the formation of thin polymer films is observed, which contain agglomerates of synthetic hydroxyapatite (Figure 1b). A detailed examination of the morphology of the biomimetic layer (Figure 1b, inset) allows us to conclude that spherical agglomerates, measuring 100-200 nm, were evenly distributed within the 6,7-DiOH-PTMDHQ layer. This size is larger than the characteristic dimensions of the nanocrystals of n-cHAp [19] used in this study to form the layer. Furthermore, the agglomerates were not merely incorporated into the 6,7-DiOH-PTMDHQ film; they were also partially enveloped by this nanopolymer.

To identify the characteristics of the deposition of individual structural elements in the biomimetic organomineral layer on the biotemplate, while considering the local chemical inhomogeneities of its morphology (Figure 2), infrared synchrotron scanning near-field optical microscopy (IR s-SNOM) with nanometer spatial resolution was used [13, 27, 28]. For signal excitation, we utilized radiation from a powerful quantum cascade infrared laser, which enabled spectral chemical mapping with a resolution of approximately 30 nm. Homogeneous areas of the samples in the enamel prism region were selected for analysis [29].

To simultaneously display the spectral-chemical features of the sample areas alongside the topology of their surfaces (Figures 2 a, b, e, f), near-field images of the optical phase and amplitude obtained from s-SNOM were visualized. These images correspond to infrared absorption and reflection from surface areas of 500×500 nm² (Figures 2 c, d, g, h). For constructing the chemical image, a resonant photon energy of 1043 cm^{-1} was utilized, which corresponds to the characteristic vibrations associated with the phosphate band ν_3 PO_4^{3-} of enamel apatite and synthesized nanocrystalline hydroxyapatite (Figures 2 c, d, g, h).

The analysis of the atomic force microscopy images of the surface topology of the reference

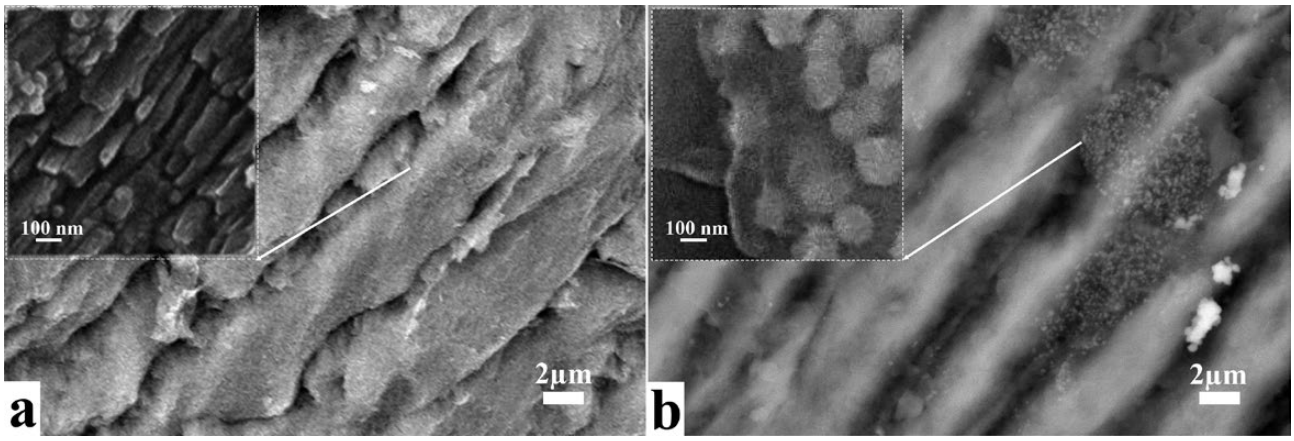

Fig. 1. SEM results. (a) natural enamel (biotemplate); (b) PTMDHQ – coating on the enamel surface based on 2,2,4-trimethyl-1,2-dihydroquinoline-6,7-diol polymerized in the presence of n-kHAp

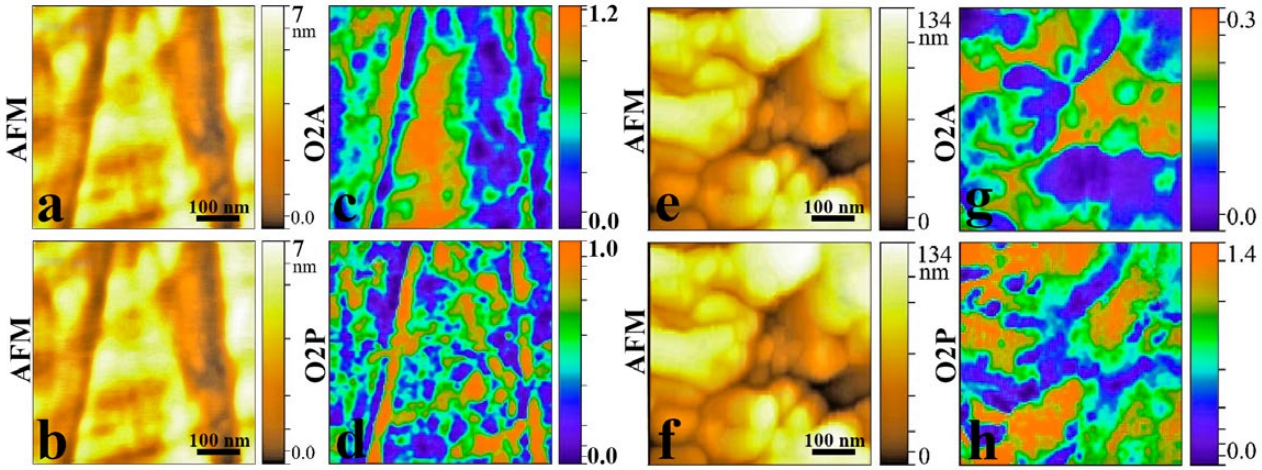

Fig. 2. Results of s-SNOM nanoimaging for a sample of natural enamel (top), PTMDHQ (bottom). For each sample, 2D AFM images of the surface topography over a 500×500 nm^2 area are simultaneously presented, as well as chemical images of these areas - the second harmonic intensity distribution for optical amplitude (O2A) and phase (O2P), corresponding to IR reflection and absorption, respectively, at resonance frequencies of 1043 cm^{-1}

sample of natural enamel (Figures 2 a, b) revealed that, despite fine polishing, grooves left by the abrasive material were still visible. The contrast obtained using infrared scattering-type near-field optical microscopy (IR s-SNOM), which reflects the distribution of phosphate groups in the dental matrix in this area (Figures 2 c, d), visualized the path of the enamel prism formed by the dense packing of apatite nanocrystals. Additionally, a sufficiently homogeneous distribution of the amino acid network was detected, which correlates with existing literature [7, 12]. From the chemical contrast image, it can be observed that the localization area of the enamel rod on the AFM topology (Figure 2b) coincides with the maximum value of the optical phase, which is proportional to the intensity of optical absorption of the mode ν_3 PO_4^{3-} at 1043 cm^{-1} (Figure 2d). The analysis of the 2D AFM topology of the PTMDHQ sample (Figures 2 d, e) demonstrates that its surface exhibits a characteristic rough morphology, formed because of the pre-treatment procedure of the enamel using orthophosphoric acid and calcium hydroxide [9], as well as the deposition of PTMDHQ. The changes in the nanorelief reached approximately 130 nm and revealed the emergence of enamel prism nanocrystals from the biotemplate surface, which became apparent after etching (Figure 2e).

Analyzing the chemical spectral images of the PTMDHQ sample, which were constructed based on the distribution of optical amplitude and phase (Figures 2g, h), it is important to note that the effective depth for useful signal extraction in the infrared s-SNOM method reached 100 nm [30]. Thus, taking into account technological data on the thickness of the deposited biomimetic layers of PTMDHQ (approximately 40 nm), the chemical contrast in the spectral images simultaneously reflects the characteristics of both the layer and the biotemplate (Figures 2g, h). PTMDHQ was deposited on the surface of biotemplates along with nanocrystals of defective n-HA, which measure approximately 20 x 50 nm and exhibit a morphological organization like that of natural enamel apatite [19, 20]. Previous studies have demonstrated that hydroxyapatite (HA) forms complexes with hydroxyquinoline via the formation of π-π bonds [31]. This leads to the formation of globular structures of varying sizes, with diameters dependent on the initial organization of hydroxyapatite. Upon analyzing the chemical images obtained using s-SNOM (Figures 2g, h), which visualize the distribution of absorption and reflection at the resonance frequency of the phosphate mode at 1043 cm^{-1}, several observations can be made. On the surface of the PTMDHQ sample, areas of localization of the phosphate mode with a radial shape were

evident (Figure 2g), indicating the presence of agglomerates (particles) of phosphates with diameters of approximately 100 nm. This finding is consistent with the results obtained from scanning electron microscopy (Figure 1b, inset). Furthermore, the maximum intensity of signal localization from the film on the s-SNOM maps coincided with the peak absorption of the phosphate mode at 1043 cm^{-1}, corresponding to the emergence of enamel prisms of apatite. Thus, the analysis of s-SNOM data suggests that calcium phosphate globules, surrounded by an organic shell and incorporated into the structure of the biomimetic film at varying depths, have formed on the surface of the PTMDHQ sample. A compact structure consisting of PTMDHQ/n-cHAp particles, uniformly distributed across the enamel surface and forming a continuous layer, has been established.

To determine the mechanical properties of the biomimetic layers based on PTMDHQ, which were deposited in the presence of nanocrystalline hydroxyapatite on the enamel surface, microhardness tests were conducted using the Vickers method. A slice of healthy enamel without an organomineral layer (biotemplate) was used as a reference sample. The results of Vickers microhardness measurements (VHN) at a load of 50 g and a loading time of 10 seconds indicated that the VHN for the healthy enamel sample (biotemplate) was 362±21, while for the biomimetic organomineral layers of PTMDHQ, the VHN was 322±26. The comparison of these values with known literature data for healthy enamel, which was reported as 338±16 [32], revealed that the VHN for the PTMDHQ sample was only 10% lower than that of healthy natural enamel.

The data obtained suggest the potential for using PTMDHQ/n-cHAp to create new hybrid biocoatings on the enamel surface. Additionally, they underscore the necessity for further research focused on enhancing the mechanical properties of the developed biomimetic layers.

4. Conclusion

The study presents the results of research on a biomimetic organomineral layer composed of trimethyldihydroquinoline polymerized in the presence of nanocrystalline, carbonate-substituted, non-stoichiometric hydroxyapatite. The morphological features of the biomimetic layer were visualized using near-field synchrotron infrared spectroscopy.

It has been demonstrated that the biomimetic layer formed on the surface of dental enamel exhibits a morphological structure characterized by a uniformly distributed and densely packed composite film of poly(2,2,4-trimethyl-1,2-dihydroquinoline-6,7-diol) and n-cHAp. Furthermore, the dental coating developed from polydihydroxyquinoline and nanocrystalline hydroxyapatite possesses a Vickers hardness coefficient comparable to that of healthy enamel.

Contribution of the authors

The authors contributed equally to this article.

Conflict of interests

The authors declare that they have no known competing financial interests or personal relationships that could have influenced the work reported in this paper.

References

1. Setlur A. S., Karunakaran C., Anusha V., ... Kusanur R. Investigating the molecular interactions of quinoline derivatives for antibacterial activity against bacillus subtilis: computational biology and in vitro study interpretations. *Molecular Biotechnology*. 2024;66: 3252–3273. https://doi.org/10.1007/s12033-023-00933-6

2. Wang R., Cao Y., Jia D., Liu L., Li F. New approach to synthesize 8-hydroxyquinoline-based complexes with Zn^{2+} and their luminescent properties. *Optical Materials*. 2013;36: 232–237. https://doi.org/10.1016/j.optmat.2013.08.032

3. Abeydeera N., Benin B. M., Mudarmah K., ... Huang S. D. Harnessing the dual antimicrobial mechanism of action with Fe(8-Hydroxyquinoline)3 to develop a topical ointment for mupirocin-resistant MRSA infections. *Antibiotics*. 2023;12: 886. https://doi.org/10.3390/antibiotics12050886

4. Nowicki J., Jaroszewska K., Nowakowska-Bogdan E., Szmatoła M., Iłowska J. Synthesis of 2,2,4-trimethyl-1,2-*H*-dihydroquinoline (TMQ) over selected organosulfonic acid silica catalysts: selectivity aspects. *Molecular Catalysis*. 2018;454: 94–103. https://doi.org/10.1016/j.mcat.2018.05.016

5. Kumar G., Sathe A., Krishna V. S., Sriram D., Jachak S. M. Synthesis and biological evaluation of dihydroquinoline carboxamide derivatives as anti-tubercular agents. *European Journal of Medicinal Chemistry*. 2018;157: 1–13. https://doi.org/10.1016/j.ejmech.2018.07.046

6. Ball V. Composite materials and films based on melanins, polydopamine, and other catecholamine-based materials. *Biomimetics*. 2017;2: 12. https://doi.org/10.3390/biomimetics2030012

7. Seredin P., Goloshchapov D., Emelyanova A., ... Mahdy I. A. Rapid deposition of the biomimetic hydroxyapatite-polydopamine-amino acid composite layers onto the natural enamel. *ACS Omega*. 2024. https://doi.org/10.1021/acsomega.3c08491

8. Kaushik N., Nhat Nguyen L., Kim J. H., Choi E. H., Kumar Kaushik N. Strategies for using polydopamine to induce biomineralization of hydroxyapatite on implant materials for bone tissue engineering. *International Journal of Molecular Sciences*. 2020;21(18): 6544. https://doi.org/10.3390/ijms21186544

9. Seredin P., Goloshchapov D., Kashkarov V., ... Prutskij T. Biomimetic mineralization of tooth enamel using nanocrystalline hydroxyapatite under various dental surface pretreatment conditions. *Biomimetics*. 2022;7(3): 111. https://doi.org/10.3390/biomimetics7030111

10. Teaford M. F., Smith M. M., Ferguson M. W. J. *Development, function and evolution of teeth*. Cambridge University Press; 2007.

11. Freitas R. O., Cernescu A., Engdahl A., ... Klementieva O. Nano-infrared imaging of primary neurons. *Cells*. 2021;10: 2559. https://doi.org/10.3390/cells10102559

12. Amarie S., Zaslansky P., Kajihara Y., Griesshaber E., Schmahl W. W., Keilmann F. Nano-FTIR chemical mapping of minerals in biological materials. *Beilstein Journal of Nanotechnology*. 2012;3: 312–323. https://doi.org/10.3762/bjnano.3.35

13. Seredin P., Goloshchapov D., Peshkov Y., ... Freitas R. O. Identification of chemical transformations in enamel apatite during the development of fissure caries at the nanoscale by means of synchrotron infrared nanospectroscopy: a pilot study. *Nano-Structures; Nano-Objects*. 2024;38: 101205. https://doi.org/10.1016/j.nanoso.2024.101205

14. López E. O., Rossi A. L., Bernardo P. L., Freitas R. O., Mello A., Rossi A. M. Multiscale connections between morphology and chemistry in crystalline, zinc-substituted hydroxyapatite nanofilms designed for biomedical applications. *Ceramics International*. 2019;45: 793–804. https://doi.org/10.1016/j.ceramint.2018.09.246

15. Seredin P., Goloshchapov D., Kashkarov V., ... Prutskij T. Development of a visualisation approach for analysing incipient and clinically unrecorded enamel fissure caries using laser-induced contrast imaging, micro-Raman spectroscopy and biomimetic composites: a pilot study. *Journal of Imaging*. 2022;8: 137. https://doi.org/10.3390/jimaging8050137

16. Goloshchapov D. L., Kashkarov V. M., Ippolitov Y. A.; Prutskij T., Seredin P. V. Early screening of dentin caries using the methods of micro-Raman and laser-induced fluorescence spectroscopy. *Results in Physics*. 2018;10: 346–347. https://doi.org/10.1016/j.rinp.2018.06.040

17. Seredin P., Goloshchapov D., Prutskij T., Ippolitov Y. Phase transformations in a human tooth tissue at the initial stage of caries. *PLoS ONE*. 2015;10: e0124008. https://doi.org/10.1371/journal.pone.0124008

18. Goloshchapov D., Buylov N., Emelyanova A., ...Seredin P. Raman and XANES spectroscopic study of the influence of coordination atomic and molecular environments in biomimetic composite materials integrated with dental tissue. *Nanomaterials*. 2021;11: 3099. https://doi.org/10.3390/nano11113099

19. Goloshchapov D. L., Minakov D. A., Domashevskaya E. P., Seredin P. V. Excitation of luminescence of the nanoporous bioactive nanocrystalline carbonate-substituted hydroxyapatite for early tooth disease detection. *Results in Physics*. 2017;7: 3853–3858. https://doi.org/10.1016/j.rinp.2017.09.055

20. Goloshchapov D. L., Lenshin A. S., Savchenko D. V., Seredin P. V. Importance of defect nanocrystalline calcium hydroxyapatite characteristics for developing the dental biomimetic composites. *Results in Physics*. 2019;13: 102158. https://doi.org/10.1016/j.rinp.2019.102158

21. Nakayama M., Kajiyama S., Kumamoto A., ... Kato T. Stimuli-responsive hydroxyapatite liquid crystal with macroscopically controllable ordering and magneto-optical functions. *Nature Communications*. 2018;9: 568. https://doi.org/10.1038/s41467-018-02932-7

22. Ocelic N., Huber A., Hillenbrand R. Pseudoheterodyne detection for background-free near-field spectroscopy. *Applied Physics Letters*. 2006;89: 101124. https://doi.org/10.1063/1.2348781

23. Keilmann F., Hillenbrand R. Near-field microscopy by elastic light scattering from a tip. *Philosophical Transactions of the Royal Society of London. Series A: Mathematical, Physical and Engineering Sciences*. 2004;362: 787–805. https://doi.org/10.1098/rsta.2003.1347

24. Beniash E., Stifler C. A., Sun C.-Y., ... Gilbert P. U. P. A. The hidden structure of human enamel. *Nature Communications*. 2019;10: 4383. https://doi.org/10.1038/s41467-019-12185-7

25. Free R., DeRocher K., Cooley V., Xu R., Stock S. R., Joester D. Mesoscale structural gradients in human tooth enamel. *Proceedings of the National Academy of Sciences*. 2022;119: e2211285119. https://doi.org/10.1073/pnas.2211285119

26. Besnard C., Marie A., Sasidharan S., ... Korsunsky A. M. Synchrotron X-ray studies of the structural and functional hierarchies in mineralised human dental enamel: a state-of-the-art review. *Dentistry Journal*. 2023;11: 98. https://doi.org/10.3390/dj11040098

27. Huth F., Govyadinov A., Amarie S., Nuansing W., Keilmann F., Hillenbrand R. Nano-FTIR absorption spectroscopy of molecular fingerprints at 20 nm spatial resolution. *Nano Letters*. 2012;12: 3973–3978. https://doi.org/10.1021/nl301159v

28. Mester L., Govyadinov A. A., Chen S., Goikoetxea M., Hillenbrand R. Subsurface chemical nanoidentification by nano-FTIR spectroscopy. *Nature Communications*. 2020;11: 3359. https://doi.org/10.1038/s41467-020-17034-6

29. Freitas R. O., Deneke C., Maia F. C. B., ... Westfahl H. Low-aberration beamline optics for synchrotron infrared nanospectroscopy. *Optics Express*. 2018;26: 11238. https://doi.org/10.1364/OE.26.011238

30. Muller E. A., Pollard B., Bechtel H. A., Van Blerkom P., Raschke M. B. Infrared vibrational nanocrystallography and nanoimaging. *Science Advances*. 2016;2: e1601006. https://doi.org/10.1126/sciadv.1601006

31. Matsuya T., Otsuka Y., Tagaya M., Motozuka S., Ohnuma K., Mutoh Y. Formation of stacked luminescent complex of 8-hydroxyquinoline molecules on hydroxyapatite coating by using cold isostatic pressing. *Materials Science and Engineering: C*. 2016;58: 127–132, https://doi.org/10.1016/j.msec.2015.08.020

32. Chuenarrom C., Benjakul P., Daosodsai P. Effect of indentation load and time on knoop and vickers microhardness tests for enamel and dentin. *Materials Research*. 2009;12: 473–476. https://doi.org/10.1590/S1516-14392009000400016

Information about the authors

Pavel V. Seredin, Dr. Sci. (Phys.–Math.), Full Professor, Chair of Department of Solid State Physics and Nanostructures, Voronezh State University (Voronezh, Russian Federation).
https://orcid.org/0000-0002-6724-0063
paul@phys.vsu.ru

Dmitry L. Goloshchapov, Cand. Sci. (Phys.–Math.), Assistant Professor, Department of Solid State Physics and Nanostructures, Voronezh State University (Voronezh, Russian Federation).
https://orcid.org/0000-0002-1400-2870
goloshchapov@phys.vsu.ru

Yaroslav A. Peshkov, Laboratory Research Assistant, Department of Solid State Physics and Nanostructures, Voronezh State University (Voronezh, Russian Federation).
https://orcid.org/0000-0003-0939-0466
tangar77@mail.ru

Nikita S. Buylov, Cand. Sci. (Phys.–Math.), Assistant Professor, Department of Solid State Physics and Nanostructures, Voronezh State University (Voronezh, Russian Federation).
https://orcid.org/0000-0003-1793-4400
buylov@phys.vsu.ru

Andrey Yu. Potapov, Cand. Sci. (Chem.), Senior Researcher at the Department of the Organic Chemistry, Voronezh State University (Voronezh, Russian Federation).
https://orcid.org/0000-0001-8084-530X
pistones@mail.ru

Khidmet S. Shikhaliev, Dr. Sci. (Chem.), Professor, Head of the Department of Organic Chemistry, Voronezh State University (Voronezh, Russian Federation).
https://orcid.org/0000-0002-6576-0305
chocd261@chem.vsu.ru

Yury A. Ippolitov, Dr. Sci. (Med.), Full Professor, Head of Dentistry Institute of Postgraduate Medical Education Department, Voronezh State Medical University (Voronezh, Russian Federation).
https://orcid.org/0000-0001-9922-137X
dsvgma@mail.ru

Raul O. Freitas, Channel Manager, Brazilian Synchrotron Light Laboratory (LNLS), Brazilian Center for Research in Energy and Materials (CNPEM), Campinas 13083-970 (Sao Paulo, Brazil).
https://orcid.org/0000-0002-3285-5447
raul.freitas@lnls.br

Francisco C. B. Maia, Research Fellow, Brazilian Synchrotron Light Laboratory (LNLS), Brazilian Center for Research in Energy and Materials (CNPEM), Campinas 13083-970 (Sao Paulo, Brazil).
https://orcid.org/0000-0002-4998-4624
francisco.maia@lnls.br

Received April 7, 2025; accepted after reviewing April 30, 2025; accepted for publication May 15, 2025; published online September 25, 2025.